5-2017

Using an Altimeter-derived Internal Tide Model to Remove Tides from In Situ Data

Edward D. Zaron
Portland State University, ezaron@pdx.edu

Richard D. Ray
NASA Goddard Space Flight Laboratory

Citation Details

Zaron, E. D., & Ray, R. D. (2017). Using an altimeter-derived internal tide model to remove tides from in situ data. Geophysical Research Letters, 44(9), 4241-4245, doi:10.1002/2017GL072950.

AGU PUBLICATIONS

Geophysical Research Letters

RESEARCH LETTER
10.1002/2017GL072950

Key Points:
- Steric height and surface velocity are predicted by an empirical M_2 internal tide model and compared with in situ data
- Use of the model as a tide correction leads to positive variance reduction
- Scaling the steric height prediction to account for the level of no motion increases the explained variance

Correspondence to:
E. D. Zaron,
ezaron@pdx.edu

Citation:
Zaron, E. D., and R. D. Ray (2017), Using an altimeter-derived internal tide model to remove tides from in situ data, *Geophys. Res. Lett.*, *44*, 4241–4245, doi:10.1002/2017GL072950.

Received 2 DEC 2016
Accepted 31 MAR 2017
Accepted article online 6 APR 2017
Published online 14 MAY 2017

Using an altimeter-derived internal tide model to remove tides from in situ data

Edward D. Zaron[1] **and Richard D. Ray**[2]

[1]Department of Civil and Environmental Engineering, Portland State University, Portland, Oregon, USA, [2]NASA Goddard Space Flight Laboratory, Greenbelt, Maryland, USA

Abstract Internal waves at tidal frequencies, i.e., the internal tides, are a prominent source of variability in the ocean associated with significant vertical isopycnal displacements and currents. Because the isopycnal displacements are caused by ageostrophic dynamics, they contribute uncertainty to geostrophic transport inferred from vertical profiles in the ocean. Here it is demonstrated that a newly developed model of the main semidiurnal (M_2) internal tide derived from satellite altimetry may be used to partially remove the tide from vertical profile data, as measured by the reduction of steric height variance inferred from the profiles. It is further demonstrated that the internal tide model can account for a component of the near-surface velocity as measured by drogued drifters. These comparisons represent a validation of the internal tide model using independent data and highlight its potential use in removing internal tide signals from in situ observations.

1. Introduction

Internal waves at tidal periods, i.e., the internal tides, are often prominent signals in oceanic data [*Wunsch*, 1975]. Most ocean measurements with profiling instruments and drifters are obtained at a temporal resolution which is insufficient to resolve tides, and tidal variability in these observations is aliased to lower frequencies. One consequence of this aliasing is that the vertical displacements of water mass properties caused by tides can cause significant errors in the geostrophic velocity inferred using the thermal wind relation [*Moum et al.*, 1987; *Johns et al.*, 1989]. Tidal currents at the ocean surface can also be significant [*Poulain and Centurioni*, 2015] and lead to difficulties in the analysis of near-inertial variability in surface drifter data [*Elipot et al.*, 2016].

The purpose of the present note is to explore the degree to which an altimeter-derived model for the low-mode internal tide can be used to predict the internal tide observed in vertical profiles of water mass properties and in surface drifter velocities. Measurements from satellite altimeters and inferences from ocean models indicate that while the internal tide wave field is spatially variable, it is at least partly coherent with the astronomical tide generating force [*Ray and Mitchum*, 1996; *Simmons et al.*, 2004] and can be mapped over a large fraction of the global oceans [*Dushaw et al.*, 2011; *Ray and Zaron*, 2016; *Zhao et al.*, 2016]. Here the predicted surface elevation caused by the internal tide is compared with steric height inferred from two sets of profile data, and the predicted tidal current is compared with surface drifter data. In each case the tide model is found to explain a positive fraction of the observed data variance.

2. Data and Methods

The internal tide model used in the present application was developed from harmonic analysis of approximately 25 years of satellite altimeter measurements of sea surface height. The surface expression of the internal tide is only a few centimeters in amplitude, and long time series, accurate corrections for the surface tide, subtidal sea level, and other processes are required to map it [*Ray and Zaron*, 2016]. The model used here includes only the largest, and most precisely known, M_2 component of the internal tide.

Three data sets are used for the comparisons of tidal predictions with in situ data. The first data set consists of 1497 temperature, salinity, and depth profiles obtained as part of the Argo Program to measure properties throughout the global oceans [*Roemmich et al.*, 2009]. The subset of these data used were collected near the Hawaiian Ridge during the period 2005 to 2015 (Figure 1a). Only data meeting the highest quality control criteria and collected by Sounding Oceanographic Lagrangian Observer, hereafter referred to as SOLO, floats are used. For comparison with the tide model the profiles are converted to steric height of the ocean surface with

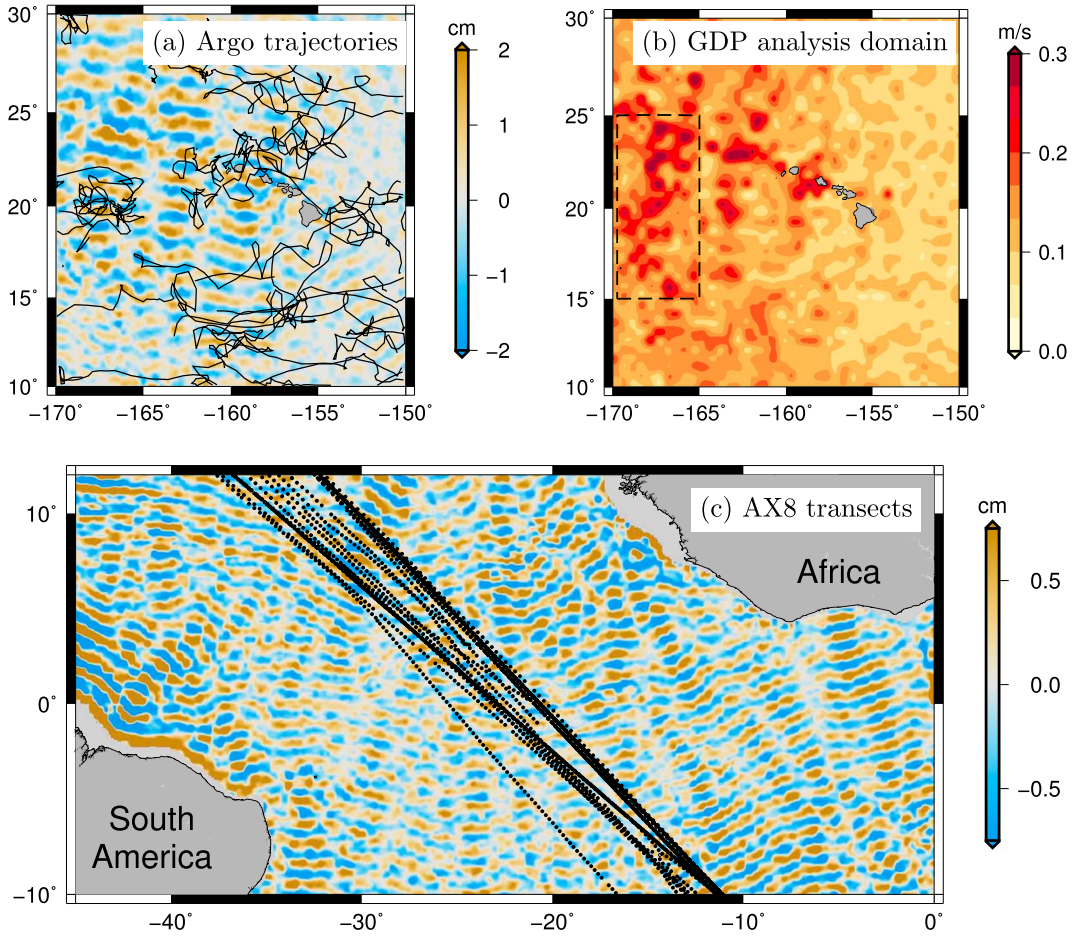

Figure 1. Data locations. (a) Argo trajectories near the Hawaiian Ridge (black). Map shows a snapshot of elevation from the M_2 internal tide model. (b) Dashed box shows the Global Drifter Program (GDP) data analysis domain. Map shows the RMS semidiurnal tidal current speed inferred from the surface drifters using the methodology of *Poulain and Centurioni* [2015]. (c) Locations of the XBT casts along the AX8 transects (black dots) in a subset of the analysis domain (20°S–20°N). Note that the color scale was chosen to illustrate the tide near the AX8 transects, and it is saturated at many locations closer to the coast.

respect to 500 m depth. The domain of the comparison (10°N–30°N, 170°W–150°W) was chosen because the amplitude of the internal tide is relatively large within it, and because it contains enough profiles to stably estimate the explained variance.

The second data set consists of 379,060 hourly surface current vectors inferred from drogued drifters deployed between 2005 and 2015 by the Global Drifter Program (GDP) [*Elipot et al.*, 2016] within a subset of the region above (15°N–25°N, 170°W–165°W). Currents are predicted from the internal tide model by assuming that the surface velocity vector, $\mathbf{u} = (u, v)$, is related to the gradient of the complex tidal surface elevation, η, using the momentum equations, $-i\omega\mathbf{u} + f\hat{k} \times \mathbf{u} = -g\nabla\eta$, where ω is the frequency of the M_2 tide, f is the Coriolis parameter, g is gravitational acceleration, and u and v are, respectively, the eastward and northward velocity components. Note that the barotropic tidal currents in this region are very small and are not included in the comparison. The spatial density of the drifter data is sufficient to map the semidiurnal tidal amplitude [*Poulain and Centurioni*, 2015], and the inferred tidal currents exhibit a similar pattern of decay away from the Hawaiian Ridge as found in the altimeter-derived model (Figure 1b). Because of the large number of observations, a smaller analysis domain is used for comparison with the *Elipot et al.* [2016] velocity estimates (indicated by the dashed rectangle in Figure 1b), but tests in other nearby domains (not shown) led to results similar to those shown below.

The third data set comes from a region of much smaller internal tide variability. It consists of 25 expendable bathythermograph (XBT) transects comprising 4518 individual temperature profiles. The transects were

Table 1. Summary of Results[a]

Data Set	N	Variance Units	Data σ_d^2	Model σ_x^2	Explained $\alpha = 1$	Explained optimal α
Argo	1497	cm^2	107.0	0.58	0.35	0.37
GDP-u	6.8×10^4	$(cm/s)^2$	483.0	8.9	−2.5	na
GDP-v	6.8×10^4	$(cm/s)^2$	367.0	18.2	14.5	na
AX8	4518	cm^2	22.3	0.15	0.02	0.05

[a]The last two columns report the variance explained by the tide model *without* ($\alpha = 1$) and *with* rescaling (optimal α) using $\alpha = 0.8$ and $\alpha = 0.6$ for the Argo and AX8 data, respectively. N indicates the number of profiles or velocity observations used to compute the variance; na = not applicable.

conducted in the Atlantic two to four times per year beginning in 2002, along the AX8 line (Figure 1c) [*Goni and Baringer*, 2002]. Data were screened for obvious anomalies, and those associated with nonmonotonically increasing pressure records were excluded. Steric height is computed relative to 500 m from observed temperature and pressure in combination with climatological salinity from the World Ocean Atlas [*Antonov et al.*, 2010]. Measurement error and the use of climatological salinity result in approximately a 3 cm error in the steric height [*Goni and Baringer*, 2002].

In order to compare the observations with the model, the tidal prediction is computed at the location and time of the corresponding observation. For the AX8 data the time is recorded by a data logger when the XBT is launched off the side of the vessel and there is little ambiguity in the time of the profile, which has a duration of approximately 2.5 min (M. Baringer, personal communication, 2016). In contrast, the Argo SOLO floats rise at approximately 0.1 m/s (D. Roemmich and N. Zilberman, personal communication, 2016), and a 500 m profile takes about 5000 s to complete, or 40° of M_2 tidal phase. Attempts to account for the difference between the recorded and mean time of the Argo profiles did not lead to statistically significant improvement in agreement, so the recorded time is simply used for the tide predictions.

Because the steric height is referenced to 500 m, rather than the level of no motion, the computed steric height is a fraction of the actual steric height at the ocean surface. For any particular internal mode, the ratio of computed steric height (referenced to a given depth, z_r) versus actual steric height (referenced to the level of no motion) is given by

$$\alpha = 1 - F_{pn}(z = z_r)/F_{pn}(z = 0), \tag{1}$$

where F_{pn} is the nth pressure eigenmode, following the notation of *Hendershott* [1981]. For mode-1, the $z_r = 500$ m surface is always above the level of no motion and the coefficient α is in the range of 0.3 to 0.7 in the Atlantic and 0.6 to 0.8 in the Pacific. These values were determined by computing the vertical modes for full-water-column conductivity-temperature-depth (CTD) casts from World Ocean Circulation Experiment (WOCE) data near the AX8 and Argo profiles [*Talley*, 2007; *Koltermann et al.*, 2011]. In principle, a reference level correction factor could be estimated individually for each cast, but this is problematic both because the correction depends on the modal content, which is unknown, and because estimates of α from individual profiles are surprisingly noisy, with changes of 15% frequently occurring between adjacent stations. Thus, instead of attempting to estimate α separately for each cast, optimal constant values are found for each of the data sets, below.

3. Results

Table 1 summarizes the results in the form of variance reduction statistics. For each of the data sets a fraction of the variance is explained by the tide model, commensurate with the size of the internal tide in each case.

Because the tidal variance is a small fraction of the total variance for the data sets used here, it is important to understand the influence of sampling error on the explained variance statistics. To this end, represent the observed data, d, as the sum of a deterministic tidal signal, x, plus a random component, ϵ, which is the sum of measurement noise and nontidal signals. Assuming d and x have been demeaned, the explained variance is given by $\delta^2 = \overline{d^2} - \overline{(d-x)^2}$, or $\delta^2 = \overline{x^2} + 2\overline{\epsilon x}$, where the overline represents the mean value. The expected error

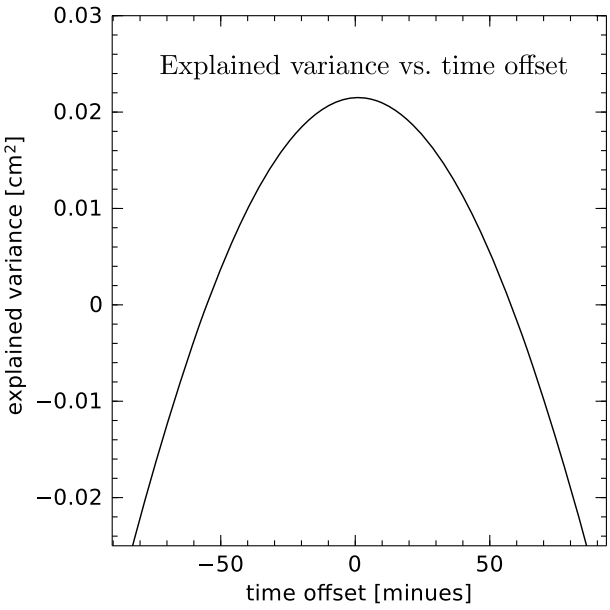

Figure 2. Explained variance of AX8 steric height is sensitive to an artificial time offset between observed and predicted tides.

of δ^2 is given by $2\sigma_\epsilon\sigma_x/\sqrt{N}$, where N is the sample size and σ_ϵ^2 and σ_x^2 are the variances of ϵ and x, respectively. Using the values provided in Table 1, and the approximation $\sigma_\epsilon = \sigma_d$, one finds the standard error of the explained variance is 0.3 cm^2, 0.4 (cm/s)^2, and 0.04 cm^2, for the ARGO, GDP, and AX8 data sets, respectively. Note that this reasoning about the standard error is based on the conservative assumption that the data are entirely random, so the standard error is thus overestimated.

For the Argo data the observed steric height variance, 107 cm^2, is the result of both spatial and temporal variability, and it is much larger than the internal tide variance, 0.58 cm^2. The tidal model explains 0.35 cm^2 of steric height variance (Table 1). When the prediction is optimally scaled by $\alpha = 0.8$, the ratio of explained-to-predicted tidal variance, δ^2/σ_x^2, is 1 and corresponds to a peak-to-peak M_2 internal tide surface displacement of 1.7 cm.

The velocity variance for the GDP data depends on direction and is reported for the zonal (GDP-u) and meridional (GDP-v) components in Table 1. Both the observed and modeled internal tide currents are anisotropic. In this case 14.5 (cm/s)^2 velocity variance is explained for the meridional component, but the explained variance is negative for the zonal component. The creation of the tide model involves filtering the altimeter data in a manner which could alter zonal gradients of η [*Ray and Zaron*, 2016] and is likely responsible for the poor performance for the zonal current. Experiments with data in other regions near the Hawaiian Ridge found a similar disparity between the statistics for the zonal and meridional velocity components (not shown).

The AX8 transects pass through a region of relatively low mesoscale and internal tide variability, and the repeated casts permit the identification of a latitude-dependent time-mean which has been used to compute a steric height anomaly. The steric height anomaly variance, 22.3 cm^2, is again much larger than the M_2 internal tide variance, 0.15 cm^2. The variance explained by the tide model is only 2e−2 cm^2; however, if the tide prediction is scaled by $\alpha = 0.6$, the explained variance is increased to 5e−2 cm^2 and the ratio of explained-to-predicted tidal variance increases to 0.9.

Note that the explained variance for the AX8 data set is only slightly larger than its standard error for the case of optimal $\alpha = 0.6$. A detailed analysis of statistical significance is probably not possible or warranted since it would depend on assumptions about the probability distribution of nontidal signals and errors, neither of which are stationary in time or space. To qualitatively assess the significance, the explained variance was recomputed after introducing an artificial time lag between the observation and the model prediction. As expected, the predicted tide is sensitive to a timing offset, and the explained variance is optimized at essentially zero lag (Figure 2). Similar exercises with the Argo and GDP data lead to the same result (not shown).

4. Discussion

Near-global maps of internal tides are now available from several researchers [*Dushaw*, 2015; *Ray and Zaron*, 2016; *Zhao et al.*, 2016]. These maps have been created using different methodologies, but they have so far been validated and quantitatively assessed primarily via comparison with altimeter data. The present comparison extends the validation effort to more diverse data and indicates a potential application for these models outside the altimeter community.

There have been many studies that demonstrate the consistency between satellite altimeter measurements of sea surface height and in situ measurements of steric height [*Gilson et al.*, 1998] and related quantities such

as vertical average sound speed [*Picaut et al.*, 1995]. The new component of this study is that it demonstrates that altimeter-derived information can predict an internal tide signal which would otherwise not be known at the time and location of the in situ observation. Negative results were obtained when comparing with the zonal velocity component of GDP data and also when data from Argo APEX floats were used (not shown). These negative results are being more systematically investigated to identify and understand the data quality and processing deficiencies leading to these outcomes.

It was noted in section 3 that the explained variance could be increased by rescaling the tidal steric height predictions with a factor, α, which partly accounts for the difference between the reference level and the level of no motion. Because values of α diagnosed directly from individual profiles may be unreliable, constant values of α were found for each data set by optimizing the explained variance, and these values were found to be within the range predicted from full-water-column CTD profiles. Nonetheless, there are additional factors which might lead to a misscaling of the tide predictions, such as the finite duration of the vertical profiles and the nature of the boundary conditions in internal wave dynamics [*Wunsch*, 2013], and these factors should be investigated in the future using larger data sets.

5. Summary

A model for the sea surface expression of the M_2 internal tide based on altimetry has been used to reduce the tidal contamination of in situ profile and surface current data. The variance explained is small but commensurate with the amplitude of the baroclinic tide. Future work will investigate the possibility of correcting the vertical profiles directly in order to reduce the gravity wave contamination of geostrophic current transects.

Acknowledgments
This work would not have been possible without the open distribution of many high-quality data sets, and the efforts of the professionals involved in the collection and dissemination of these data are gratefully acknowledged. The altimeter data are distributed as a component of the Radar Altimeter Database System (RADS, http://rads.tudelft.nl/rads/rads.shtml). The Argo data are collected and made freely available by the International Argo Program and the national programs that contribute to it (http://www.argo.ucsd.edu, http://argo.jcommops.org). The Argo Program is part of the Global Ocean Observing System. The AX8 XBT data are made freely available on the Atlantic Oceanographic and Meteorological Laboratory website and are funded by the NOAA Office of Climate Observations (http://www.aoml.noaa.gov/phod/hdenxbt/hdenxbt_intr.php). The surface drifter data are available at the Global Drifter Program website (http://www.aoml.noaa.gov/phod/dac/gdp_information.php). Full-column CTD profiles are available at the WOCE Atlas Hydrographic Program website (http://woceatlas.ucsd.edu/) and were used for the computation of vertical modes and derived quantities. This project was supported by NASA award NNX09AF20G, Ocean Surface Topography Science Team, "Studies of Surface and Internal Tides."

References

Antonov, J. I., D. Seidov, T. P. Boyer, R. A. Locarnini, A. V. Mishonov, H. E. Garcia, O. K. Baranova, M. M. Zweng, and D. R. Johnson (2010), Salinity, in *World Ocean Atlas 2009*, vol. 2, edited by S. Levitus, p. 184, NOAA Atlas NESDIS 68, U.S. Governt. Printing Office, Washington, D. C.

Dushaw, B., (2015), An empirical model for mode-1 internal tides derived from satellite altimetry: Computing accurate tidal predictions at arbitrary points over the world oceans, Tech. Rep. APL-UW TM 1-15, Univ. of Washington Applied Physics Laboratory, Seattle, Wash.

Dushaw, B. D., P. F. Worcester, and M. A. Dzieciuch (2011), On the predictability of mode-1 internal tides, *Deep Sea Res., Part I*, *58*, 677–698.

Elipot, S., R. Lumpkin, R. C. Perez, J. M. Lilly, J. J. Early, and A. M. Sykulski (2016), A global surface drifter data set at hourly resolution, *J. Geophys. Res. Oceans*, *121*, 2937–2966, doi:10.1002/2016JC011716.

Gilson, J. D., D. Roemmich, B. Cornuelle, and L.-L. Fu (1998), Relationship of TOPEX/Poseidon altimetric height to steric height and circulation in the North Pacific, *J. Geophys. Res.*, *103*, 27,947–27,965, doi:10.1029/98JC01680.

Goni, G., and M. Baringer (2002), Ocean surface currents in the Tropical Atlantic across high density XBT line AX08, *Geophys. Res. Lett.*, *29*(24), 2218, doi:10.1029/2002GL015873.

Hendershott, M. C. (1981), Long waves and ocean tides, in *Evolution of Physical Oceanography*, edited by M. C. Hendershott, pp. 293–341, MIT Press, Cambridge, Mass.

Johns, E., D. R. Watts, and H. T. Rossby (1989), A test of geostrophy in the Gulf Stream, *J. Geophys. Res.*, *94*, 3211–3222, doi:10.1029/JC094iC03p03211.

Koltermann, K. P., V. V. Gouretski, and K. Jancke (2011), Hydrographic Atlas of the World Ocean Circulation Experiment (WOCE), in *Atlantic Ocean*, vol. 3, edited by M. Sparrow, P. Chapman, and J. Gould, Int. WOCE Proj. Off., Southampton, U. K. [Available at http://www-pord.ucsd.edu/whp_atlas/atlantic_index.html.]

Moum, J. N., T. K. Chereskin, M. M. Park, and L. A. Regier (1987), Monitoring geostrophic currents at the equator, *Deep Sea Res., Part A*, *34*(7), 1149–1161.

Picaut, J., A. J. Busalacchi, M. J. McPhaden, L. Gourdeau, F. I. Gonzalez, and E. C. Hackert (1995), Open-ocean validation of TOPEX/POSEIDON sea level in the western equatorial Pacific, *J. Geophys. Res.*, *100*(C12), 25,109–25,127, doi:10.1029/95JC02128.

Poulain, P.-M., and L. Centurioni (2015), Direct measurements of World Ocean tidal currents with surface drifters, *J. Geophys. Res. Oceans*, *120*, 6986–7003, doi:10.1002/2015JC010818.

Ray, R. D., and G. T. Mitchum (1996), Surface manifestation of internal tides generated near Hawaii, *Geophys. Res. Lett.*, *23*, 2101–2104, doi:10.1029/96GL02050.

Ray, R. D., and E. D. Zaron (2016), M_2 internal tides and their observed wavenumber spectra from satellite altimetry, *J. Phys. Oceanogr.*, *46*, 3–22.

Roemmich, D., G. C. Johnson, S. Riser, R. Davis, J. Gilson, W. B. Owens, S. L. Garzoli, C. Schmid, and M. Ignaszewski (2009), The Argo program: Observing the global oceans with profiling floats, *Oceanography*, *22*, 24–33.

Simmons, H. L., R. W. Hallberg, and B. K. Arbic (2004), Internal wave generation in a global baroclinic tide model, *Deep Sea Res., Part II*, *51*, 3043–3068.

Talley, L. D. (2007), Hydrographic Atlas of the World Ocean Circulation Experiment (WOCE), in *Pacific Ocean*, vol. 2, edited by M. Sparrow, P. Chapman, and J. Gould, Int. WOCE Proj. Off., Southampton, U. K. [Available at http://www-pord.ucsd.edu/whp_atlas/pacific_index.html.]

Wunsch, C. (1975), Internal tides in the ocean, *Rev. Geophys.*, *13*(1), 167–182.

Wunsch, C. (2013), Baroclinic motions and energetics as measured by altimeters, *J. Atmos. Oceanic Technol.*, *30*, 140–150.

Zhao, Z., M. H. Alford, J. B. Girton, L. Rainville, and H. L. Simmons (2016), Global observations of open-ocean mode-1 M2 internal tides, *J. Phys. Oceanogr.*, *46*, 1657–1684.